

Complementarity Between Hyperkamiokande and DUNE in Determining Neutrino Oscillation Parameters

Shinya Fukasawa,^{*} Monojit Ghosh,[†] and Osamu Yasuda[‡]

Department of Physics, Tokyo Metropolitan University, Hachioji, Tokyo 192-0397, Japan

Abstract

In this work we investigate the sensitivity to the neutrino mass hierarchy, the octant of the mixing angle θ_{23} and the CP phase δ_{CP} in the future long baseline experiments T2HK and DUNE as well as in the atmospheric neutrino observation at Hyperkamiokande (HK). We show for the first time that the sensitivity is enhanced greatly if we combine these three experiments. Our results show that the hierarchy sensitivity of both T2HK and HK are limited due to the presence of parameter degeneracy. But this degeneracy is removed when T2HK and HK are added together. With T2HK+HK (DUNE), the neutrino mass hierarchy can be determined at least at 5σ (8σ) C.L. for any value of true δ_{CP} . With T2HK+HK+DUNE the significance of the mass hierarchy increases to almost 15σ for the unfavorable value of δ_{CP} . For these combined setup, octant can be resolved except $43.5^\circ < \theta_{23} < 48^\circ$ at 5σ C.L. for both the hierarchies irrespective of the value of δ_{CP} . The significance of CP violation is around 10σ C.L. for $\delta_{CP} \sim \pm 90^\circ$. Apart from that these combined facility has the capability to discover CP violation for at least 68% fraction of the true δ_{CP} values at 5σ for any value of true θ_{23} . We also find that, with combination of all these three, the precision of Δm_{eff}^2 , $\sin^2 \theta_{23}$ and δ_{CP} becomes 0.3%, 2% and 20% respectively. We also clarify how the octant degeneracy occurs in the HK atmospheric neutrino experiment.

^{*}e-mail: fukasawa-shinya@ed.tmu.ac.jp

[†]e-mail: monojt@tmu.ac.jp

[‡]e-mail: yasuda@phys.se.tmu.ac.jp

I. INTRODUCTION

With the discovery of the mixing angle θ_{13} by the reactor experiments [1–3], the physics of neutrino oscillation has entered into an era of precision measurement. In the standard three flavor scenario, the phenomenon of neutrino oscillation can be parametrized by three mixing angles: θ_{12} , θ_{23} and θ_{13} , two mass squared difference: Δm_{21}^2 and Δm_{31}^2 , and one Dirac type phase δ_{CP} . Thanks to the neutrino experiments in the last two decades, the values of the three mixing angles and the values of the mass squared differences are now determined in the three flavor mixing framework to some precision [4–6]. The unknown quantities at present are: (i) the mass hierarchy or the sign of Δm_{31}^2 (NH: normal hierarchy i.e., $\Delta m_{31}^2 > 0$ or IH: inverted hierarchy i.e., $\Delta m_{31}^2 < 0$), (ii) the octant of θ_{23} (LO: lower octant i.e., $\theta_{23} < 45^\circ$ or HO: higher octant i.e., $\theta_{23} > 45^\circ$) and (iii) the CP phase δ_{CP} . There are several experiments which are dedicated to determine these above mentioned unknowns.

The main difficulty in determining those unknowns is the presence of parameter degeneracy [7–11]. In parameter degeneracy, different sets of oscillation parameter leads to the same value of the oscillation probability. Due to this the true solutions can be mimicked by the false solutions and thus a unique determination of the parameters becomes difficult. One of the ways to overcome this degeneracy is to combine data from different experiments. As the degenerate parameter space is different for different experiments, combination of different experiments can lead to the removal of the fake solutions which may help in the unambiguous determination of the neutrino oscillation parameters. Recently, this strategy has been adopted by many to study the synergy between different on-going as well as future proposed experiments in determining the remaining unknowns of the neutrino oscillation parameter. In this regard, the well established method is to combine the data of the long-baseline and atmospheric neutrino oscillation experiments. The sensitivity to the remaining unknown parameters in long-baseline experiments comes from the appearance channel probabilities $P(\nu_\mu \rightarrow \nu_e)$ and $P(\bar{\nu}_\mu \rightarrow \bar{\nu}_e)$ while the atmospheric experiments can have sensitivity for both appearance and disappearance channel probabilities $P(\nu_\mu \rightarrow \nu_\mu)$ and $P(\bar{\nu}_\mu \rightarrow \bar{\nu}_\mu)$. In addition to that some of the authors also prefer to add the reactor data which has the sensitivity of the electron antineutrino disappearance channel ($\bar{\nu}_e \rightarrow \bar{\nu}_e$). Thus the combination of the long-baseline and atmospheric experiments along with the information of the precise value of θ_{13} , is believed to remove the degenerate solutions and measure the current unknowns at a significant confidence level. In Refs. [12–14], the combined analysis on the CP sensitivity of the long-baseline exper-

iments T2K [15], NO ν A [16] and atmospheric experiment ICAL@INO [17] has been studied in detail. The combined analysis on the octant sensitivity of these experiments can be found in [18]. In these analyses, the reactor information has been taken into account in the form of prior on $\sin^2 2\theta_{13}$. The hierarchy sensitivity of T2K, NO ν A and ICAL@INO along with the combination of the reactor experiments has been done in [19]. The sensitivity of the long-baseline experiment LBNO [20] with the addition of T2K, NO ν A and ICAL@INO has been studied in [21]. The combined analysis on the octant sensitivity of the atmospheric experiment PINGU [22] along with T2K, NO ν A and reactor data has been studied in Ref. [23]. The synergistic study on the hierarchy sensitivity of PINGU by combining reactor experiment has been done in [24] whereas the same with combining beam based experiments and reactors is carried out in [25]. The synergy of the proposed long-baseline experiment DUNE [26], combining both the beam and atmospheric data along with T2K, NO ν A is analyzed in [27, 28]. The combined sensitivity of DUNE in conjunction with T2K, NO ν A and ICAL@INO has been explored in [29]. All these studies shows that, the sensitivity of an individual experiment is significantly enhanced when added with the other experiments.

In this paper, for the first time we study the joint sensitivity of the long-baseline experiments T2HK [30], DUNE and the atmospheric experiment HK [31] in determining the remaining unknowns in neutrino oscillation sector. This is the so-called HK and LBNF complementarity which has been discussed in the literature [32]. We take this opportunity to work out the physics potential of these facilities in detail. The T2HK experiment is an upgrade of the ongoing T2K experiment which will use a detector to have a volume almost 25 times larger than the existing T2K detector. HK is the atmospheric counterpart of the T2HK experiment. On the other hand DUNE is a high statistics beam based experiment to use high beam power, large detector volume and longer baseline. Among all other existing facilities, these above mentioned experiments are the most promising future experiments in terms of both statistics and matter effect which have the maximum potential to reveal the true nature of the neutrino oscillation parameters. In this work we study: (i) the sensitivity of the T2HK, HK and DUNE experiments, (ii) the synergy between the T2HK and HK experiments to resolve the parameter degeneracy in the neutrino oscillation, (iii) how far the sensitivities in determining hierarchy, octant and CP can be stretched when all these three powerful experiments are combined together and (iv) the precision measurements of θ_{23} , δ_{CP} and Δm_{31}^2 of this setup.

The paper is organized as follows. In Sect. II, we describe a little about parameter degeneracy,

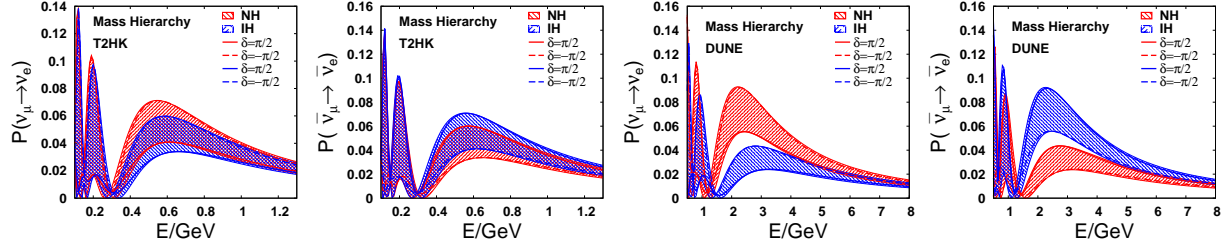


FIG. 1: The behaviors of the appearance probabilities $P(\nu_\mu \rightarrow \nu_e)$ (first and third panels) and $P(\bar{\nu}_\mu \rightarrow \bar{\nu}_e)$ (second and fourth panels) for T2HK (left two panels) and DUNE (right two panels) in the two different mass hierarchies. The width of each band comes from the degree of freedom of δ_{CP} , and the edge is approximately represented by $\delta_{CP} = \pm 90^\circ$. $\theta_{23} = 45^\circ$ is assumed in all the four figures.

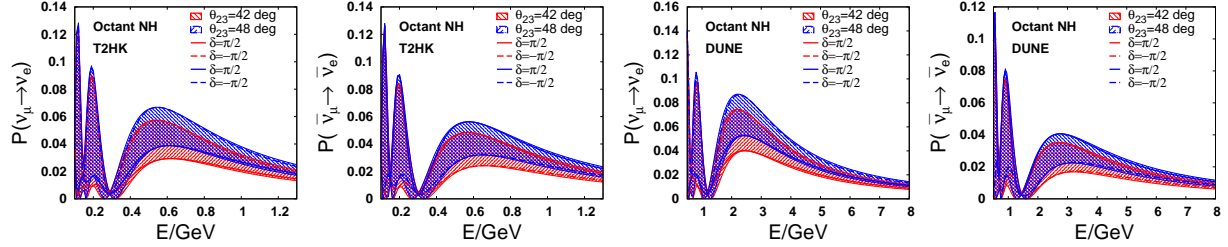


FIG. 2: The behaviors of the appearance probabilities $P(\nu_\mu \rightarrow \nu_e)$ (first and third panels) and $P(\bar{\nu}_\mu \rightarrow \bar{\nu}_e)$ (second and fourth panels) for T2HK (left two panels) and DUNE (right two panels) in the two different octants, where $\theta_{23} = 42^\circ$ or $\theta_{23} = 48^\circ$ is taken as a reference value. Normal hierarchy is assumed in all the four figures. The width of each band comes from the degree of freedom of δ_{CP} , and the edge is approximately represented by $\delta_{CP} = \pm 90^\circ$.

which becomes important for determination of the CP phase, and the experiments T2HK, DUNE and the atmospheric neutrino measurement at Hyperkamiokande (HK). In Sect. III, we give our simulation details and the results of our analysis. In Sect. IV, we draw our conclusions. In the appendix A, we provide a discussion regarding the parameter degeneracy in the HK atmospheric neutrino experiment.

II. PRELIMINARIES

A. Parameter degeneracy

The ultimate goal of the research on neutrino oscillations in the standard three flavor mixing scheme is the determination of δ_{CP} , since it is expected to be relevant to the baryon asymmetry

of the universe. It has been known that the determination of δ_{CP} is not easy because of so-called parameter degeneracy: Even if we know the values of the appearance oscillation probabilities $P(\nu_\mu \rightarrow \nu_e)$ and $P(\bar{\nu}_\mu \rightarrow \bar{\nu}_e)$ precisely, we cannot determine the oscillation parameters uniquely. Earlier when θ_{13} was not known precisely, there were three kinds of parameter degeneracy. The first parameter degeneracy is the intrinsic degeneracy [7], which occurs because the appearance oscillation probabilities are approximately quadratic in $\sin 2\theta_{13}$ for small θ_{13} and we obtain the two solutions $(\theta_{13}, \delta_{CP})$ and $(\theta'_{13}, \delta'_{CP})$. This intrinsic degeneracy is not expected to cause a problem because we now know the value of θ_{13} from the precise measurements of θ_{13} by the reactor neutrino experiments [1–3]. The second one is the sign degeneracy [8]. At this moment we do not know whether the mass hierarchy is normal or inverted. Depending on whether the mass hierarchy is normal or inverted, the appearance oscillation probabilities vary, and ignorance of the mass hierarchy may give us a completely wrong region for δ_{CP} . Thus the determination of the mass hierarchy is important for the measurement of δ_{CP} . The third one is the octant degeneracy [9]. The main contribution to the probabilities $1 - P(\nu_\mu \rightarrow \nu_\mu)$ and $1 - P(\bar{\nu}_\mu \rightarrow \bar{\nu}_\mu)$ is proportional to $\sin^2 2\theta_{23}$, and we can only determine $\sin^2 2\theta_{23}$ from the disappearance channel. If θ_{23} is not maximal, then we have two possibilities $\cos 2\theta_{23} > 0$ and $\cos 2\theta_{23} < 0$, so this ambiguity gives us two solutions $(\theta_{23}, \delta_{CP})$ and $(90^\circ - \theta_{23}, \delta'_{CP})$. The octant degeneracy can create a source of the uncertainty in θ_{23} , so its resolution is important for precise measurement of θ_{23} . These three types of degeneracies together created a eight fold degeneracy degeneracy [10] when the precise value of θ_{13} was unknown. After the discovery of θ_{13} , now the eight fold degeneracy breaks into a four fold degeneracy. At present the relevant degeneracy in the neutrino oscillation probability is known as the “generalized hierarchy-octant- δ_{CP} degeneracy” [11]. This generalized degeneracy consists of hierarchy- δ_{CP} degeneracy [33] and octant- δ_{CP} degeneracy [34] which we discuss in the next section for the T2HK and DUNE baselines.

B. T2HK and DUNE

T2HK is the long baseline experiment which is planned in Japan, and its baseline length and peak energy is $L=295$ km, $E \sim 0.6$ GeV, respectively. On the other hand, DUNE is another long baseline experiment which is planned in USA, and its baseline length and peak energy is $L=1300$ km, $E \sim 3$ GeV, respectively. The matter effect appears in the neutrino oscillation probability typically in the form of $G_F N_e L / \sqrt{2} = [\rho / (2.6 \text{ g/cm}^3)] [L / (4000 \text{ km})]$. The baseline length of T2HK

is too short for the matter effect so T2HK has poor sensitivity to the mass hierarchy. Hence the sign degeneracy can be in principle serious in determination of δ_{CP} at T2HK. On the other hand, the baseline length of DUNE is comparable to the typical length which is estimated by the matter effect, so DUNE is expected to be sensitive to the mass hierarchy.

As was discussed in the case of T2K and NO ν A in Ref. [33], we can see whether this so called hierarchy- δ_{CP} degeneracy can be resolved or not by looking at the behaviors of the appearance channel probabilities. In Fig. 1, we plot the appearance channel probability spectrum for a fixed value of $\theta_{23} = 45^\circ$. The first and second panels are for neutrino and antineutrino probabilities of T2HK and the third and fourth panels are for neutrino and antineutrino probabilities of DUNE respectively. In each panel, the red band correspond to NH and the blue band corresponds to IH. The width of the band is due to the variation of the phase δ_{CP} . The overlap region between the red band and the blue band correspond to the hierarchy- δ_{CP} degeneracy. From the Fig. 1 we see that that in the case of $\delta_{CP} = -90^\circ$ with the normal mass hierarchy (NH) or $\delta_{CP} = 90^\circ$ with the inverted mass hierarchy (IH), T2HK can resolve the mass hierarchy by the neutrino mode $\nu_\mu \rightarrow \nu_e$ alone. These are the favorable values of δ_{CP} where there is no hierarchy- δ_{CP} degeneracy. On the other hand, in the case of $\delta_{CP} = 90^\circ$ with the normal mass hierarchy or $\delta_{CP} = -90^\circ$ with the inverted mass hierarchy, we see that T2HK cannot resolve the mass hierarchy even if we combine the neutrino mode $\nu_\mu \rightarrow \nu_e$ and the antineutrino mode $\bar{\nu}_\mu \rightarrow \bar{\nu}_e$, because the curve for $\delta_{CP} = 90^\circ$ with NH or $\delta_{CP} = -90^\circ$ with IH lies in the middle of the overlapping region in the both modes. These are the unfavorable values of δ_{CP} which suffers from the hierarchy- δ_{CP} degeneracy. For the case of DUNE, though the behavior of the appearance channel probabilities are the same as that of T2HK, but the NH and IH bands are quite well separated. For this reason it is possible to have hierarchy sensitivity in DUNE even for the unfavorable parameter values of δ_{CP} .

On the other hand, the situation of the octant degeneracy is different. As shown in [34], one can identify the octant- δ_{CP} degenerate parameter space by looking at the appearance channel probabilities. In Fig. 2 we plot the same as that of Fig. 1 but for a fixed value of Δm_{31}^2 . We assume the normal mass hierarchy for simplicity. In these plots the red band corresponds to LO ($\theta_{23} = 42^\circ$) and the blue band correspond to HO ($\theta_{23} = 48^\circ$). The width of the bands are due to the variation of δ_{CP} . From Fig. 2 we see that, in the case of $\delta_{CP} = 90^\circ$, if θ_{23} lies in the first octant (i.e., if $\theta_{23} = 42^\circ$), then both T2HK and DUNE can resolve the octant degeneracy by the neutrino mode $\nu_\mu \rightarrow \nu_e$ alone, and if θ_{23} lies in the second octant (i.e., if $\theta_{23} = 48^\circ$), then T2HK and DUNE can resolve the octant degeneracy by the antineutrino mode $\bar{\nu}_\mu \rightarrow \bar{\nu}_e$ alone. This argument also

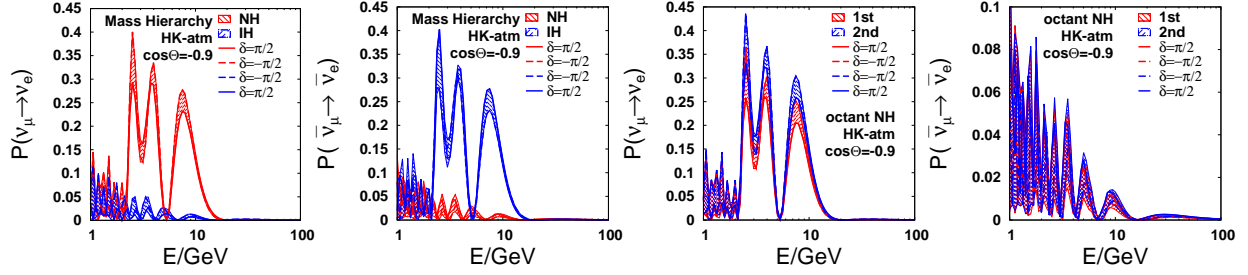


FIG. 3: The behaviors of the appearance probabilities $P(\nu_\mu \rightarrow \nu_e)$ (first and third panels) and $P(\bar{\nu}_\mu \rightarrow \bar{\nu}_e)$ (second and fourth panels) for the atmospheric neutrino measurements for the zenith angle $\cos \Theta = -0.9$ for the two different mass hierarchies (left two panels) and in the two different octants (right two panels). In the right two panels $\theta_{23} = 42^\circ$ or $\theta_{23} = 48^\circ$ is taken as a reference value, and Normal hierarchy is assumed.

applies to the case of $\delta_{CP} = -90^\circ$, and we conclude that both T2HK and DUNE has potential to resolve the octant degeneracy by themselves by combining the neutrino and antineutrino modes. These conclusions also hold for the inverted hierarchy ¹.

C. Atmospheric neutrinos

The measurement of atmospheric neutrinos at Hyperkamiokande (HK) gives us information which is complimentary to long-baseline experiments. Its advantage is that we can get the information on the oscillation probabilities for wide ranges of the neutrino energy and the baseline length, particularly for more than 4000 km, so the measurement gives us information on the matter effect. On the other hand, its disadvantages are that there are uncertainties on the baseline length, that it is difficult to distinguish neutrinos and antineutrinos, and that the oscillation probability has to be deduced indirectly from the measured flux, because the measured flux $F(\nu_\alpha) = F_0(\nu_e)P(\nu_e \rightarrow \nu_\alpha) + F_0(\nu_\mu)P(\nu_\mu \rightarrow \nu_\alpha)$ ($\alpha = e, \mu$) is the sum of the each flux which are produced out of the original flux $F_0(\nu_\alpha)$ ($\alpha = e, \mu$) through neutrino oscillations.

In our simulation of the atmospheric neutrino measurements at Hyperkamiokande, the data which is most sensitive to the mass hierarchy and the octant degeneracy is the e-like multi-GeV events ² in the higher energy region for the zenith angle $-1.0 < \cos \Theta < -0.8$. The disappearance

¹ Note that our discussion of degeneracy is valid only for a fixed value of energy E . In the realistic scenario the nature of these degeneracies can be different due to the energy dependence of the probability spectrum.

² In the multi-GeV energy region (~ 10 GeV), the ratio of the original e-like flux $F_0(\nu_e)$ to the original μ -like

probability $P(\nu_e \rightarrow \nu_e)$ is insensitive to the matter effect, so what makes the difference between the two mass hierarchies is the appearance probability $P(\nu_\mu \rightarrow \nu_e)$. In Fig. 3, the appearance probabilities are plotted for $\cos \Theta = -0.9$. The first two panels are similar as that of Fig. 1 and the third and fourth panels are similar as that of Fig. 2. From the first two panels, it is clear that as far as the appearance probabilities are concerned, we should be able to determine the mass hierarchy on the condition that we can measure the appearance probabilities for the energy and the baseline length in the atmospheric neutrino measurements. As for the octant, third panel and fourth panels of Fig. 3 suggests that the atmospheric neutrino measurements may resolve the octant degeneracy as it combines both neutrino and antineutrino probabilities.

III. ANALYSIS

A. Simulation Details

Here we assume the following parameters for each experiment:

- 1) T2HK: We have taken the parameters from Ref. [30].³

Our χ^2 is a function of the two sets of the oscillation parameters \vec{p}_{ex} and \vec{p}_{th} , and is defined as:

$$\chi_{\text{T2HK}}^2(\vec{p}_{\text{ex}}, \vec{p}_{\text{th}}) = \min_{\{\xi_j\}} \left[\chi_{\text{T2HK}}^2(\vec{p}_{\text{ex}}, \vec{p}_{\text{th}}; \{\xi_j\}) + \sum_j \left(\frac{\xi_j}{\pi^j} \right)^2 \right],$$

where $\{\xi_j\}$ are the pull variables, π^j are the (1σ) systematic errors for the pull variable ξ_j , with

$$\chi_{\text{T2HK}}^2(\vec{p}_{\text{ex}}, \vec{p}_{\text{th}}; \{\xi_j\}) = 2 \sum_i \left[M_i(\vec{p}_{\text{th}}) - N_i(\vec{p}_{\text{ex}}) + N_i(\vec{p}_{\text{ex}}) \ln \left(\frac{N_i(\vec{p}_{\text{ex}})}{M_i(\vec{p}_{\text{th}})} \right) \right]. \quad (1)$$

one $F_0(\nu_\mu)$ is approximately 1:6, so the relative contribution of the appearance probability in the total flux after oscillations is larger in the e-like flux $F(\nu_e) \sim F_0(\nu_e)\{P(\nu_e \rightarrow \nu_e) + 6P(\nu_\mu \rightarrow \nu_e)\}$ than in the μ -like one $F(\nu_\mu) \sim F_0(\nu_\mu)\{(1/6)P(\nu_e \rightarrow \nu_\mu) + P(\nu_\mu \rightarrow \nu_\mu)\}$. Therefore the e-like events are more sensitive to the mass hierarchy than the μ -like ones.

³ In the recent design of the Hyperkamiokande project [35], two tanks with the fiducial volume 0.19 Mton each with the staging construction is planned. At this moment, the details are not known, so we will analyze T2HK and the atmospheric neutrino measurements at Hyperkamiokande with the parameters in the old design of Hyperkamiokande throughout this paper.

The ‘experimental’ data $N_i(\vec{p}_{\text{ex}})$ are simulated using the ‘true’ oscillation parameters \vec{p}_{ex} , while the ‘theoretical’ events $N_i(\vec{p}_{\text{th}})$ are generated using the ‘test’ oscillation parameters \vec{p}_{th} . The subscript i here runs over all the energy bins. The theoretical events get modified due to systematic errors as

$$M_i(\vec{p}_{\text{th}}) = N_i(\vec{p}_{\text{th}}) \left[1 + \sum_k \xi_k + \sum_l \xi_l \frac{E_i - E_{\text{av}}}{E_{\text{max}} - E_{\text{min}}} \right].$$

are the theoretical numbers of events including the systematic uncertainty. Where the index $k(l)$ runs over the relevant normalization (tilt) systematic errors for a given experimental observable. The normalization errors affect the scaling of events and the tilt errors affect the energy dependence of the events. All the pull variables $\{\xi_j\}$ take values in the range $(-3\pi^j, 3\pi^j)$, so that the errors can vary from -3σ to $+3\sigma$. Here, E_i is the mean energy of the i^{th} energy bin, E_{min} and E_{max} are the limits of the full energy range, and E_{av} is their average. The final χ^2 is then calculated by minimizing over all combinations of ξ_j .

Total exposure: 1.56×10^{22} POT (protons on target). This implies, for a beam power of 1×10^{21} POT/year, it corresponds to 15.6 year running.

Flux: 30 GeV proton beam

Detector: 0.56 Mton (fiducial volume) water Čerenkov

$\nu:\bar{\nu} = 1:1$

Systematics: an overall normalization error of 3.3% for both appearance and disappearance channel in neutrino mode and 6.2% (4.5%) for appearance (disappearance) channel in antineutrino mode. The normalization error is same for both signal and background. For tilt error we have taken 1% (5%) corresponding to signal (background) in appearance channel and 0.1% in disappearance channel for both signal and background. Tilt error for neutrinos and antineutrinos are taken to be same.

For T2HK we have reproduced the sensitivity as given in Ref. [30].

2) DUNE: We have taken the parameters from Ref. [26].

In the case of the DUNE experiment χ^2 is defined as in the same manner as T2HK.

Total exposure: 1.0×10^{22} POT. Thus for a beam power of 1×10^{21} POT/year, it will run for 10 years.

Flux: 120 GeV proton beam

Detector: 34 kton (fiducial volume) Liquid Argon

$\nu:\bar{\nu} = 1:1$

Systematics: an overall normalization error of 2% (10%) for appearance channel and 5% (15%) for disappearance channel corresponding to signal (background) in both neutrino and antineutrino mode. The tilt error is 2.5%.

Our sensitivity results of DUNE are in agreement with Ref. [26].

The simulations of T2HK and DUNE have been performed with the software GLoBES [36, 37].

- 3) Atmospheric neutrino measurements at Hyperkamiokande: We have taken the parameters from Ref. [31].

Detector: 0.56 Mton (fiducial volume) water Čerenkov

Duration: 200 days \times 10 years = 2000 days

As in Ref. [38], we use the data set of the sub-GeV events with the two energy-bins, the multi-GeV events with the two energy-bins, and the combined stopping and through-going upward going μ events with the single energy-bin, where the number of the zenith angle bins is ten for all these channels.

Simulation of the atmospheric neutrino at Hyperkamiokande is done with the codes which were used in Refs. [38–41]. In our analysis, we compared our χ^2 and the value of χ^2 given by the HK collaboration in Ref. [30] and normalized our χ^2 for each analysis (mass hierarchy, octant, and CP violation) so that the two χ^2 approximately coincide with each other. Thus our sensitivity of the HK experiment matches with Ref. [30].

The analysis was performed using χ^2 -method. χ^2 depends on the two sets of the oscillation parameters \vec{p}_{ex} and \vec{p}_{th} , and is defined as

$$\begin{aligned} & \chi_{\text{atm}}^2(\vec{p}_{\text{ex}}, \vec{p}_{\text{th}}) \\ &= \min_{\theta_{23}, |\Delta m_{32}^2|, \delta, \epsilon_{\alpha\beta}} [\chi_{\text{sub-GeV}}^2(\vec{p}_{\text{ex}}, \vec{p}_{\text{th}}) + \chi_{\text{multi-GeV}}^2(\vec{p}_{\text{ex}}, \vec{p}_{\text{th}}) + \chi_{\text{upward}}^2(\vec{p}_{\text{ex}}, \vec{p}_{\text{th}})] , \quad (2) \end{aligned}$$

where $\chi_{\text{sub-GeV}}^2(\vec{p}_{\text{ex}}, \vec{p}_{\text{th}})$, $\chi_{\text{multi-GeV}}^2(\vec{p}_{\text{ex}}, \vec{p}_{\text{th}})$ and $\chi_{\text{upward}}^2(\vec{p}_{\text{ex}}, \vec{p}_{\text{th}})$ are χ^2 for the sub-GeV, muti-GeV, and upward μ events, and they are the same as $\chi_{\text{sub-GeV}}^2$, $\chi_{\text{multi-GeV}}^2$ and

χ^2_{upward} defined in Ref. [38], respectively. The way we introduce the systematic errors is an extension of that in the original analysis of atmospheric neutrinos. [42] In our code we have used the old atmospheric neutrino flux [43] instead of the new one [44], because our simulation results become closer to the ones by Superkamiokande collaboration with the old flux. However the difference in χ^2 between the old flux and the new flux is small (\sim a few %), since our simulated experimental data are also evaluated with the same flux. So the choice of the atmospheric neutrino flux does not affect our conclusions very much. We have set the systematic errors to the same values as in Ref. [45] except several unimportant factors. In particular, we confirmed that taking a uncertainty in the E_ν spectral index which is omitted in our analysis into consideration gives negligible contributions to χ^2 . See Refs. [38, 46] for further details.

In our simulation we have fixed the value of $\sin^2 \theta_{12} = 0.3$, $\sin^2 2\theta_{13} = 0.1$, $\Delta m_{21}^2 = 7.5 \times 10^{-3} \text{ eV}^2$ and $|\Delta m_{\text{eff}}^2| = 2.4 \times 10^{-3} \text{ eV}^2$. This is a good approximation since these parameters are well constrained from the global analysis from the world neutrino data [4–6] and thus marginalization over these parameters will not affect the sensitivity much. We vary θ_{23} from 40° to 50° and δ_{CP} from -180° to $+180^\circ$. For estimating the precision of θ_{23} and Δm_{eff}^2 , we have kept δ_{CP} fixed at -90° for both true and test spectrum.

B. Sensitivity of HK

In this section we study the potential of the HK experiment to determine the neutrino mass hierarchy, octant and δ_{CP} .

Fig. 4 shows the sensitivity of HK to the mass hierarchy, octant and CP violation. In the top left panel we present the hierarchy sensitivity χ^2 as a function of true δ_{CP} for the HK experiment. Hierarchy sensitivity of an experiment is defined by taking the right hierarchy in the true spectrum and wrong hierarchy in the test spectrum. While calculating χ^2 we have marginalized over θ_{23} and δ_{CP} in the test spectrum. The purple band in the figure corresponds to sensitivity in NH and the blue band corresponds to sensitivity in IH. The width of the band is due to the variation of true θ_{23}

⁴ Following Ref. [47], we adopt the effective mass squared difference for the μ disappearance channel, and it is defined as $\Delta m_{\text{eff}}^2 \equiv s_{12}^2 \Delta m_{31}^2 + c_{12}^2 \Delta m_{32}^2 + \cos \delta_{CP} s_{13} \sin 2\theta_{12} \tan \theta_{23} \Delta m_{21}^2$. We consider this in our analysis because in vacuum, the hierarchy degeneracy do not occur for $P_{\mu\mu}(\Delta m_{31}^2) = P_{\mu\mu}(-\Delta m_{31}^2)$ but it occurs for $P_{\mu\mu}(\Delta m_{\text{eff}}^2) = P_{\mu\mu}(-\Delta m_{\text{eff}}^2)$.

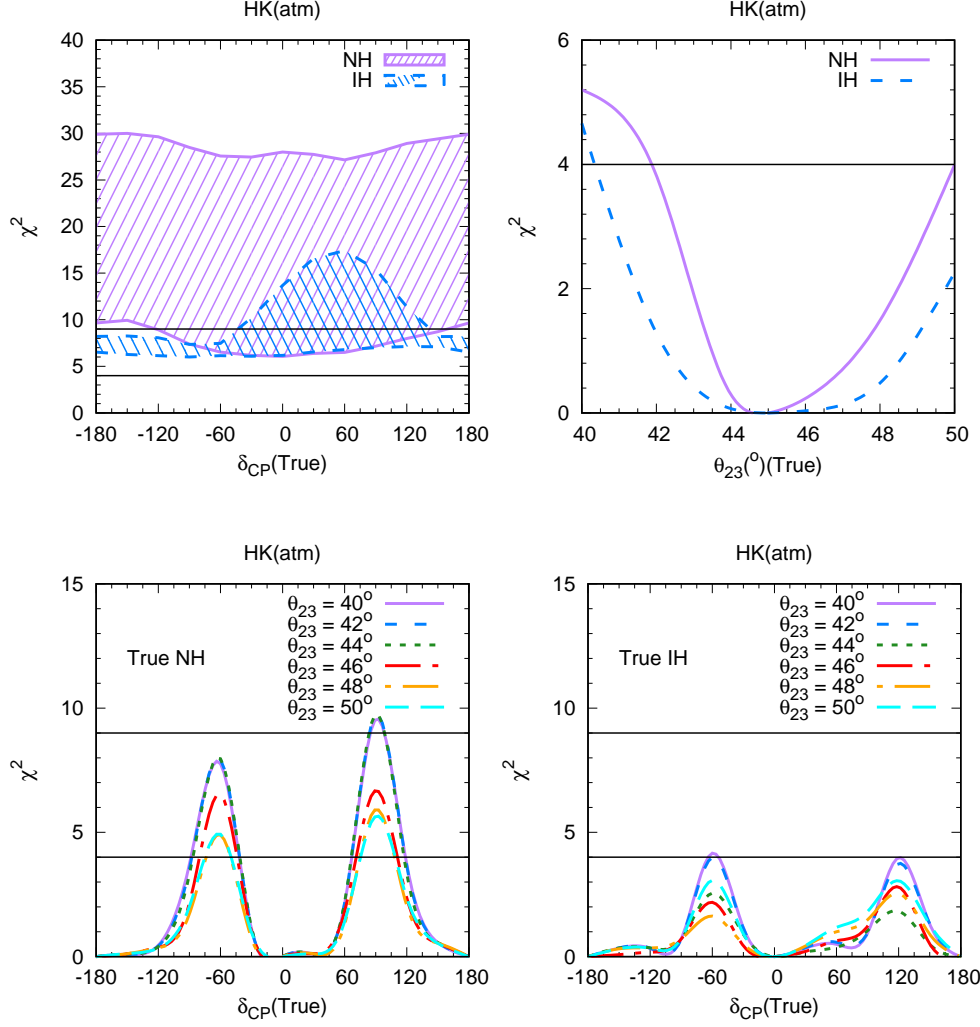


FIG. 4: Sensitivity of the HK atmospheric neutrino experiment to the mass hierarchy (the top left panel), octant (the top right panel) and CP violation (bottom row). In the top left panel the width of the band comes from the uncertainty in θ_{23} .

from 40° to 50° which is the current allowed values of θ_{23} . From the figure we observe that, for conservative value of θ_{23} ,⁵ the hierarchy χ^2 is close to 6 around $\delta_{CP} = 0^\circ$ for both NH and IH and for optimistic value of θ_{23} , the hierarchy sensitivity increases to $\chi^2 = 30$ for NH around $\pm 180^\circ$ and $\chi^2 = 18$ for IH around $\delta_{CP} = +60^\circ$. Here it is interesting to see that the hierarchy sensitivity of IH is in general poorer as compared to NH. It is also important to note that for $-180^\circ < \delta_{CP} < -60^\circ$, the width of the IH band is very narrow. This is because for water Čerenkov detectors, it has been

⁵ The word “conservative (optimistic)” means the value of θ_{23} for which the hierarchy sensitivity is minimum (maximum).

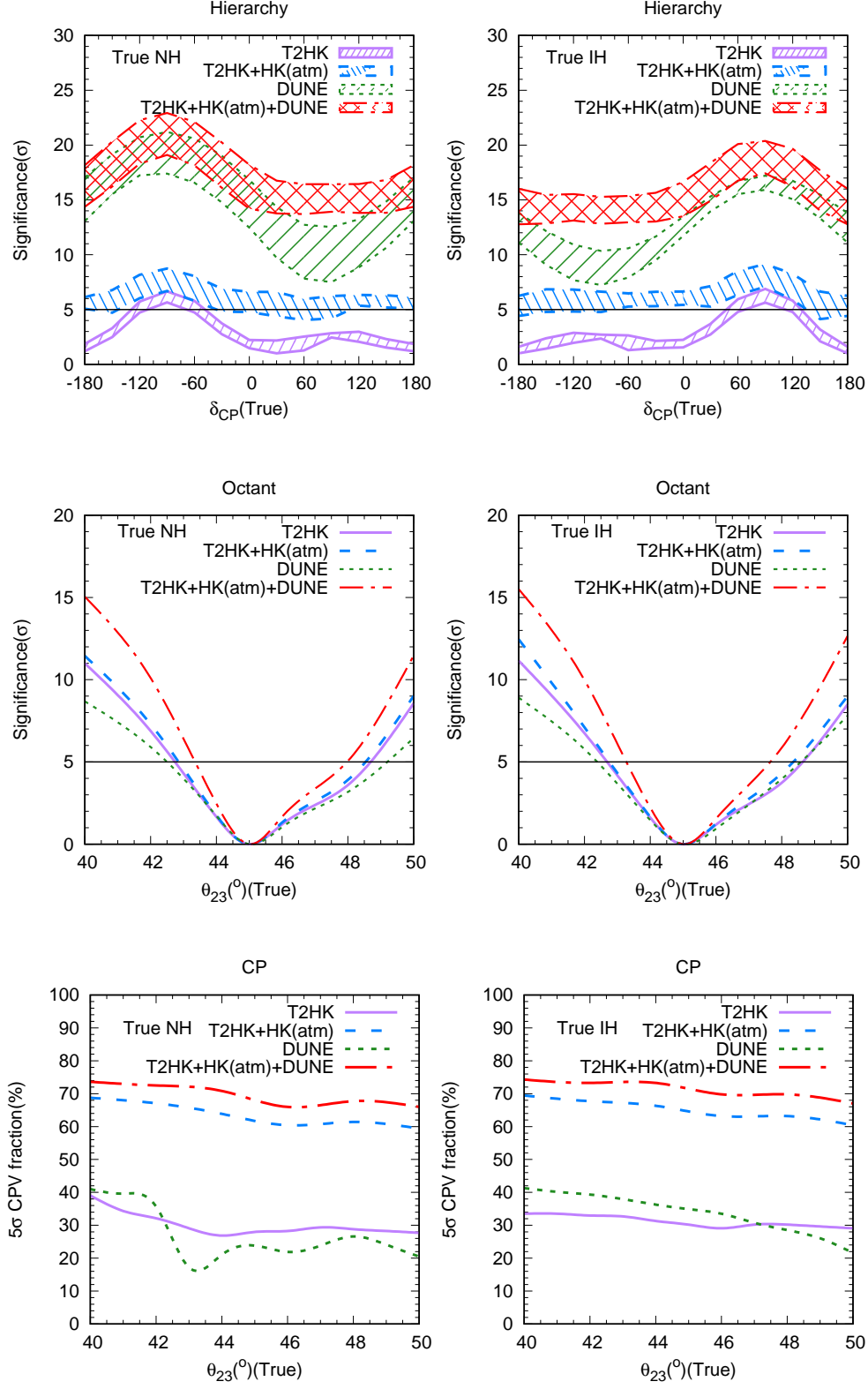


FIG. 5: Sensitivity to the mass hierarchy, octant and CP violation. In the upper and middle rows the vertical axis is $\sqrt{\chi^2}$.

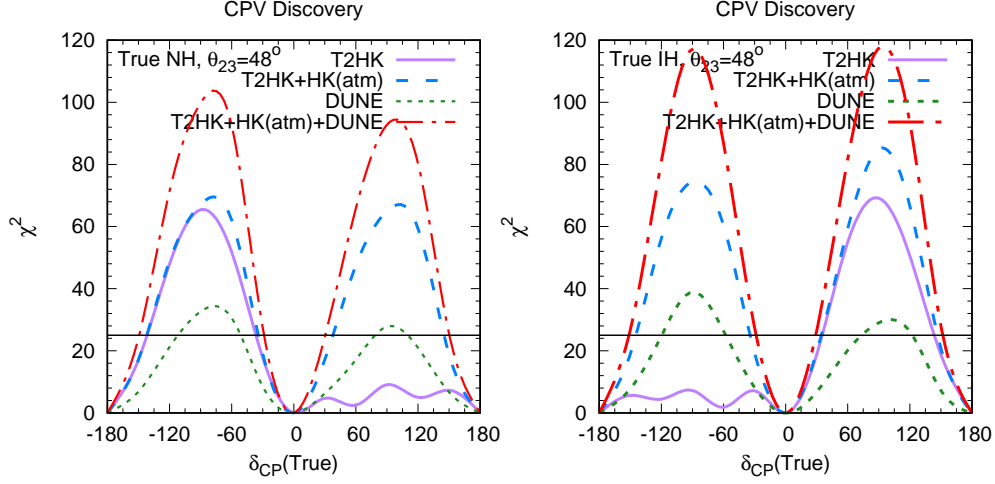


FIG. 6: Sensitivity to CP violation for $\theta_{23} = 48^\circ$.

shown that NH-LO is degenerate with IH-HO [25, 48]. Thus because of the octant degeneracy, we obtain a very poor hierarchy sensitivity for HK in IH in the above mentioned parameter space. Note that although NH is not free from this degeneracy but the degeneracy in NH seems less severe as compared to the degeneracy in IH. We will discuss this point in detail in the appendix.

In the top right panel of Fig. 4 we plot the octant χ^2 as a function of the true θ_{23} . The sensitivity to the octant is defined by taking the correct octant of θ_{23} in the true spectrum and wrong octant of θ_{23} in the test spectrum. In the process of calculating χ^2 for octant sensitivity we have marginalized over $\text{sign}(\Delta m_{\text{eff}}^2)$ and δ_{CP} in the test spectrum. The purple curve is for NH and the blue curve is for IH. In generating those plots, we have calculated octant sensitivity for each values of true δ_{CP} and choose the minimum χ^2 for given value of true θ_{23} . Thus the sensitivity reflected in the figure corresponds to the conservative values of the δ_{CP} . From the figure we see that the octant sensitivity of HK is poor. It can only determine octant if the true value of θ_{23} lies between $40^\circ - 42^\circ$ for NH at 2σ sensitivity and for IH almost the full parameter space is allowed at 2σ .

Now let us discuss the CP sensitivity of the HK experiment. In the lower row of Fig. 4, we have plotted the CP violation discovery χ^2 vs true δ_{CP} for five different true values of θ_{23} . Left panel is for NH and the right panel is for IH. The CP violation discovery potential of an experiment is defined by its capability to distinguish a true value of δ_{CP} from test value of 0° or 180° . In all our plots we have minimized the χ^2 with respect to $\text{sign}(\Delta m_{\text{eff}}^2)$ and θ_{23} in the test spectrum. From the figures we conclude that CP sensitivity in NH is higher as compared to the CP sensitivity in IH. For NH, $\theta_{23} = 40^\circ, 42^\circ$ and 44° have almost the same CP sensitivity and one can have a 3σ

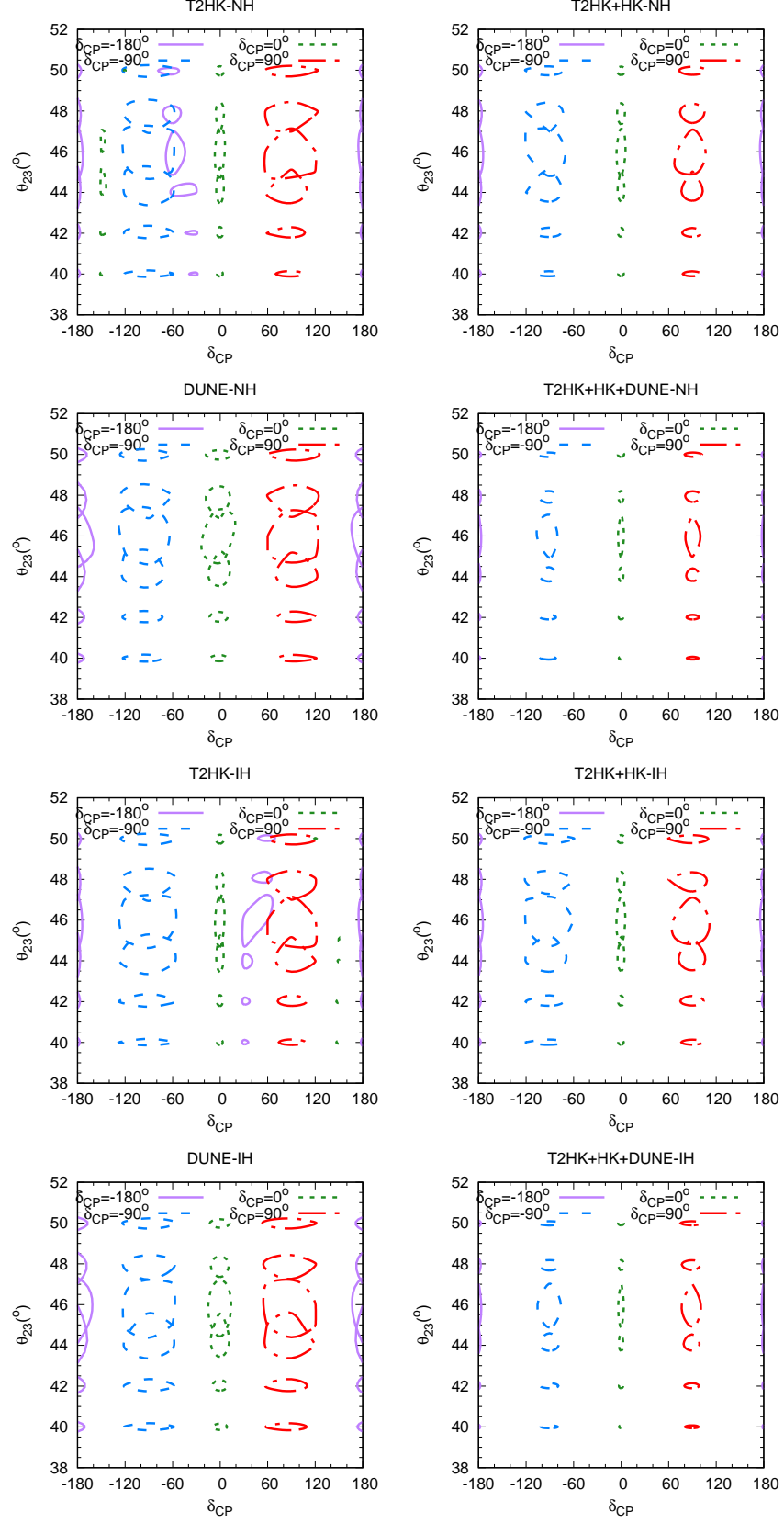


FIG. 7: 90% C.L. contour in the test δ_{CP} and test θ_{23} plane for several representative true points.

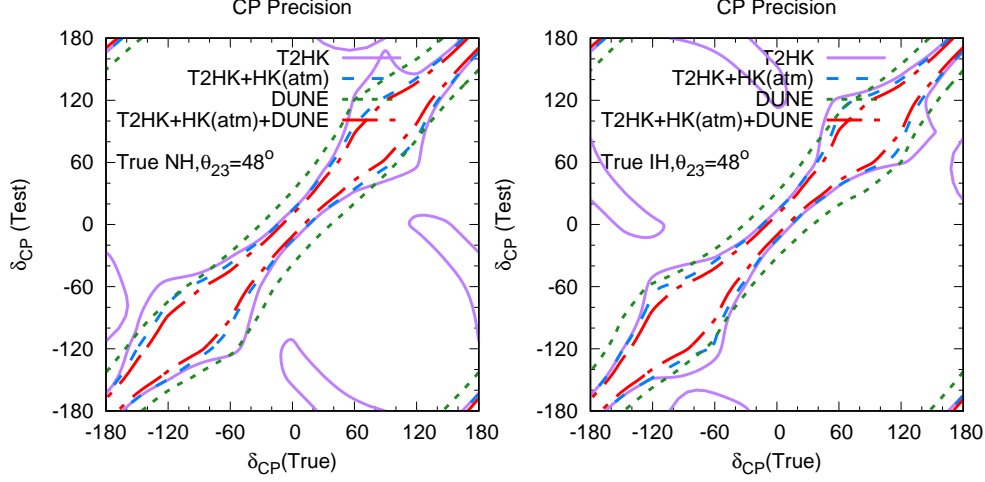


FIG. 8: The correlation of the true and test CP phases by individual experiment or by various combinations of the experiments for $\theta_{23} = 48^\circ$ at 3σ C.L.

sensitivity at $\delta_{CP} = +90^\circ$ for these θ_{23} values. Then as θ_{23} increases, CP sensitivity decreases. On the other hand, in the case of IH for $\theta_{23} = 40^\circ$ and 42° one can have a 2σ CP sensitivity around $\delta_{CP} = \pm 90^\circ$ and the for the other values CP sensitivity deteriorates due to the presence of degeneracy.

C. Combined Sensitivity of T2HK, HK and DUNE

In this section we will study the synergy between T2HK, HK and DUNE in determining the unknowns of neutrino oscillation and also study up to what confidence level these unknowns can be determined.

1. Hierarchy

In the upper row of Fig. 5, we plot the significance $\sqrt{\chi^2}$ at which hierarchy can be determined as a function of true δ_{CP} . The left panel is for true NH and the right panel is for true IH. These plots are similar as that of top left panel of Fig. 4. As it is explained in Subsect. II B, in the case of $\delta_{CP} = -90^\circ$ with NH and $\delta_{CP} = 90^\circ$ with IH, T2HK can resolve the mass hierarchy and the sensitivity of T2HK is good, whereas in the case of $\delta_{CP} = 90^\circ$ with NH and $\delta_{CP} = -90^\circ$ with IH, T2HK cannot resolve the mass hierarchy by itself, so the sensitivity of T2HK becomes poor. If we

combine T2HK and the Hyperkamiokande atmospheric neutrino data, then T2HK+HK(atm) can resolve the sign degeneracy at 5σ C.L. for any value of δ_{CP} . Here it is important to note that for IH, in the region $-180^\circ < \delta_{CP} < 0^\circ$, both T2HK and HK has poor hierarchy sensitivity. In this parameter space, T2HK suffers from hierarchy degeneracy and HK suffers from octant degeneracy. But when these experiments are combined there is a great enhancement in the sensitivity in that unfavorable values of δ_{CP} . This reflects the synergy between these two experiments which are essential to achieve a hierarchy sensitivity around 5σ C.L. irrespective of the true value δ_{CP} . On the other hand, for DUNE, the separation of the two mass hierarchies are good and DUNE itself has above 5σ C.L. sensitivity to the mass hierarchy for any value of δ_{CP} . If we combine T2HK, the HK atmospheric neutrino data and DUNE, then the significance of the mass hierarchy becomes as large as 15σ C.L., even for the unfavorable values of δ_{CP} . This is a quite remarkable result which shows the potential of these experiments to discover neutrino mass hierarchy.

2. Octant

In the middle panels of Fig. 5, we plot the significance $\sqrt{\chi^2}$ at which the wrong octant can be excluded as a function of true θ_{23} . The left panel is for true NH and the right panel is for true IH. These figures are similar as that of the top right panel of Fig. 4 i.e., our results corresponds to the conservative values of δ_{CP} . From the plots we see that the values of θ_{23} for which octant can be resolved at 5σ C.L is almost the same for T2HK, T2HK+HK and DUNE. For these setups octant can be determined except $43^\circ < \theta_{23} < 49^\circ$ for both NH and IH at 5σ C.L. However when all the three experiments are combined we see that there is a significant amount of increase in the octant sensitivity for both the hierarchies. From the figure we see that T2HK+HK+DUNE can resolve octant except $43.5^\circ < \theta_{23} < 48^\circ$ for both the hierarchies at 5σ C.L.

3. CP Violation

In the lower panels of Fig. 5 we plot the fraction of true δ_{CP} values for which CP violation can be discovered at a 5σ confidence level as function of true θ_{23} . The left panel is for NH and the right panel is for IH. From the plots we see that as θ_{23} increases the percentage of true δ_{CP} decreases. For T2HK+HK, the δ_{CP} fraction varies from 60% to 70% and for T2HK+HK+DUNE, the δ_{CP} fraction varies from 75% to 68%. From these results we clearly understand that the combination

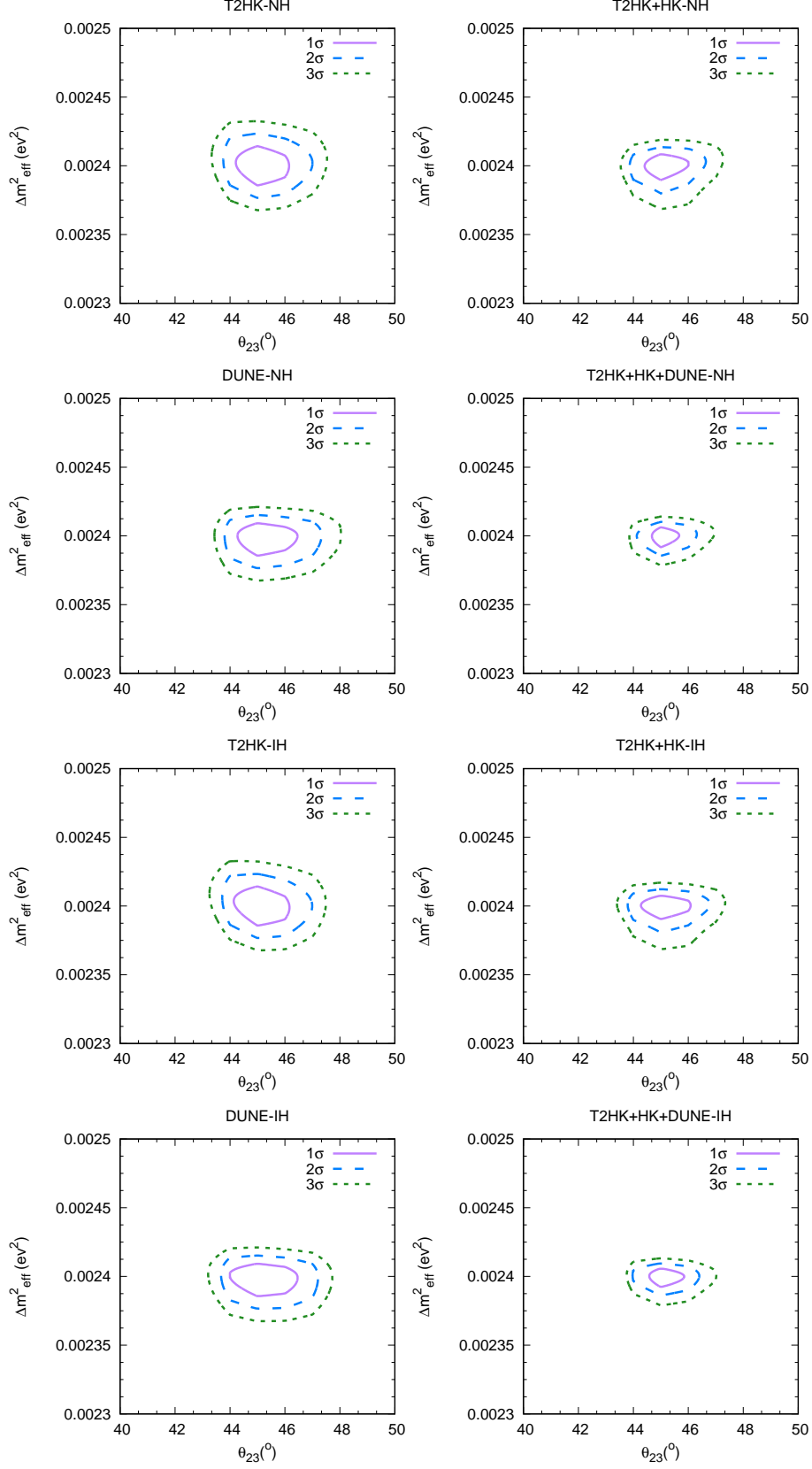


FIG. 9: The correlation between Δm^2_{eff} and θ_{23} for various combinations of the experiments. Normal (inverted) hierarchy is assumed in the first and second (third and fourth) row.

Sensitivity	T2HK	T2HK+HK(atm)	DUNE	T2HK+HK(atm)+DUNE
Hierarchy	1	5	8	15
Octant	$43^\circ - 49^\circ$	$43^\circ - 49^\circ$	$43^\circ - 49^\circ$	$43.5^\circ - 48^\circ$
CP Violation	30	60	20	68

TABLE I: Sensitivity for hierarchy, octant and CP at conservative values of the true parameter. For hierarchy, $\sqrt{\chi^2}$ is given. For octant, the region for θ_{23} which is allowed at 5σ is given. For CP violation, the fraction of δ_{CP} for which CPV can be discovered at $\chi^2 = 25$ is given in %.

of these three experiments have the capability to discover CP violation at 5σ C.L. for at least 68% true values of δ_{CP} . This is an incredible result since no other existing facilities can have such a reach to discover CP violation.

From these figures we also note that the sensitivities of DUNE and T2HK are similar. To understand this in Fig. 6, we plot the CP violation discovery χ^2 as a function of true δ_{CP} for $\theta_{23} = 48^\circ$ which is the present best-fit value of θ_{23} . As was discussed in Subsect. II B, the sensitivity of T2HK to CP is poor for $\delta_{CP} \sim 90^\circ$ with NH and $\delta_{CP} \sim -90^\circ$ with IH. On the other hand due to large matter effect DUNE has almost equal sensitivity at $\pm 90^\circ$ for both the hierarchies. But due to very high statistics, T2HK has very large CP sensitivity in the favorable values of δ_{CP} and this gives almost comparable coverage of true δ_{CP} values for which CP violation can be discovered at 5σ C.L. It is also important to note that if we combine the result of the Hyperkamiokande atmospheric neutrino data to T2HK, then sensitivity is good also for the unfavorable values of δ_{CP} . This is because the hierarchy sensitivity of HK, removes the wrong hierarchy solutions of T2HK in the unfavorable parameter space. We note in passing that synergy between T2K and the atmospheric neutrino measurement at ICAL@INO for CP violation discovery was studied in Ref. [12]. Furthermore, if we combine T2HK, the Hyperkamiokande atmospheric neutrino and DUNE, then the sensitivity to CP violation reaches around 10σ C.L. for $\delta_{CP} \sim -90^\circ$ for both NH and IH.

D. Precision of δ_{CP} , θ_{23} and Δm_{eff}^2

In this section we study how much precisely the parameters δ_{CP} , θ_{23} and Δm_{eff}^2 can be measured by the set up under consideration. In Fig. 7 we show the 90% C.L. precision contours in the test θ_{23} and test δ_{CP} plane for various true values by individual experiments or by combinations of the experiment. The true θ_{23} values are considered as 40° to 50° with a step of 2° and the true δ_{CP} values are considered as -180° to 90° with a step of 90° . The upper panels are for NH and the lower panels are for IH. Because of the difficulty of resolving the sign degeneracy at T2HK, T2HK alone may lead to wrong region for the test CP phase. This can be seen from the top left and bottom left panels of Fig. 7 which corresponds to the T2HK experiment. For true $\delta_{CP} = -180^\circ$, the wrong regions are seen around -30° ($+30^\circ$) for NH (IH). But in DUNE there are no wrong solutions at all (the top third and bottom third panels). Note that when we combine T2HK with the HK atmospheric neutrino data, then the fake region for the test CP phase disappears (the top second and bottom second panels). The precision is seen to be excellent when all the three experiments are combined (the top fourth and bottom fourth panel).

To understand the synergy between different experiments in improving the CP precision, in Fig. 8, we plot the 3σ contours in the δ_{CP} (true) vs δ_{CP} (test) plane for a fixed value of $\theta_{23} = 48^\circ$. The left panel is for NH and the right panel is for IH. From the plot we see that, for T2HK there are wrong δ_{CP} solutions mainly in the region $0^\circ < \delta_{CP} < 180^\circ$ in NH and $-180^\circ < \delta_{CP} < 0^\circ$ in IH. But when the HK is added with it, the wrong solutions completely disappears. But in the case of DUNE there are no wrong δ_{CP} solutions. It is also seen that the CP precision is excellent when all the three experiments are combined. Here it is interesting to note that the precision of δ_{CP} is better at $\delta_{CP} = 0^\circ$ as compared to $\delta_{CP} = \pm 90^\circ$.

Finally in Fig. 9 we plotted the 1σ , 2σ and 3σ contours in the $\Delta m_{\text{eff}}^2 - \theta_{23}$ plane for various combinations of the experiments. The true value is taken as $\theta_{23} = 45^\circ$ and $|\Delta m_{\text{eff}}^2| = 0.0024 \text{ eV}^2$. In generating these plots we have kept δ_{CP} fixed at -90° in both true and test spectrum. The upper panels are for NH and the lower panels are for IH. From the plots we see that T2HK and DUNE have similar sensitivity. If we combine T2HK, the HK atmospheric neutrino data and DUNE, then the errors in Δm_{eff}^2 , $\sin^2 \theta_{23}$ and δ_{CP} become 0.3%, 2% and 20%, respectively.

E. Precision of θ_{13}

In this paper we have discussed only the measurements of Δm_{eff}^2 , θ_{23} and δ_{CP} . Let us discuss briefly whether the combination of T2HK+HK+DUNE can improve the current precision on θ_{13} which is obtained by the reactor experiments. It is known [49] that if we fix the values of the both appearance probabilities $P(\nu_\mu \rightarrow \nu_e)$ and $P(\bar{\nu}_\mu \rightarrow \bar{\nu}_e)$, then it gives us a quadratic curve in the $(\sin^2 2\theta_{13}, 1/\sin^2 \theta_{23})$ plane, where a point sweeps the quadratic curve as δ_{CP} varies from 0 to 2π . The region of the quadratic curve in the $(\sin^2 2\theta_{13}, 1/\sin^2 \theta_{23})$ plane is the necessary and sufficient condition which can be obtained from the appearance probabilities $P(\nu_\mu \rightarrow \nu_e)$ and $P(\bar{\nu}_\mu \rightarrow \bar{\nu}_e)$ only. To get information on θ_{13} from this quadratic curve without the reactor data, we need to combine the disappearance probabilities $P(\nu_\mu \rightarrow \nu_\mu)$ and $P(\bar{\nu}_\mu \rightarrow \bar{\nu}_\mu)$ with the appearance probabilities. Because the error $\delta(\sin^2 \theta_{23}) = (1/4)\delta(\sin^2 2\theta_{23})/(1 - \sin^2 2\theta_{23})^{1/2}$ is enhanced due to the singular Jacobian factor at the maximal mixing [50], the uncertainty in the vertical coordinate in the $(\sin^2 2\theta_{13}, 1/\sin^2 \theta_{23})$ plane is expected to be large. Notice that the uncertainty in the horizontal coordinate $\sin^2 2\theta_{13}$ is not enhanced in the case of the reactor measurements, because $\sin^2 2\theta_{13}$ appears linearly in the disappearance probability in the reactor experiments. From this discussion, we expect that it is difficult for the combination of T2HK+HK+DUNE to give a precision on θ_{13} which is competitive with the current one from the reactor experiments.

IV. CONCLUSION

In this paper we have studied the sensitivity of T2HK, HK and DUNE to mass hierarchy, octant of the mixing angle θ_{23} and δ_{CP} . The main results of our analysis are summarized in Table I. Although it is difficult for T2HK to resolve the sign degeneracy for unfavorable region of the CP phase, when we combine it with the atmospheric neutrino measurement at Hyperkamiokande, we can determine the mass hierarchy at 5σ C.L. for any value of δ_{CP} . We have also clarified how the octant degeneracy occurs and why its behavior depends on the mass hierarchy in the HK atmospheric neutrino measurements. On the other hand, DUNE can determine the mass hierarchy at least at 8σ C.L. by itself. Furthermore, if we combined all of them, then the significance to mass hierarchy is at least 15σ C.L. In our analysis we found out that the octant sensitivity of T2HK, T2HK+HK and DUNE are quite similar in ruling out the wrong octant at 5σ C.L. But for T2HK+HK+DUNE the increase in the octant sensitivity is significant. For CP violation discovery

we find that the combination T2HK+HK can measure CP violation at 8σ C.L. for $\delta_{CP} = \pm 90^\circ$ and for T2HK+HK+DUNE the significance for CP violation is around 10σ C.L. for $\delta_{CP} = \pm 90^\circ$. It is also quite impressive that with the combination of all the three experiment CP violation can be established at 5σ C.L. for at least 68% true values of δ_{CP} . In the combination of all these experiments above, the precision in Δm_{eff}^2 , θ_{23} and δ_{CP} is 0.3%, 2% and 20%. The precision in the first two parameters is improved by one order of magnitude compared with the current data. We will be in the era of precision measurements of neutrino oscillation parameters, and combination of Hyperkamiokande and DUNE will play an important role in determination of δ_{CP} as well as θ_{23} .

Acknowledgement

MG would like to thank Srubabati Goswami for useful discussions. This work is supported by the ‘‘Grant-in-Aid for Scientific Research of the Ministry of Education, Science and Culture, Japan’’, under Grants No. 25105009, No. 15K05058, No. 25105001 and No. 15K21734.

Appendix A: Octant degeneracy in the atmospheric neutrinos

In this appendix, we will discuss the octant degeneracy in the atmospheric neutrino measurements and we will clarify the reason why the significance of the mass hierarchy differs depending on the true mass hierarchy.

The atmospheric neutrinos which can be directly measured are e-like and μ -like events and its sensitivity to the mass hierarchy can be expressed by χ^2 which is defined as⁶

$$\chi^2 = \sum_j \sum_{\beta=e,\mu} \left[\sum_{\alpha=e,\mu} \left\{ N_j^{\alpha\beta}(WH) + N_j^{\bar{\alpha}\bar{\beta}}(WH) - N_j^{\alpha\beta}(TH) - N_j^{\bar{\alpha}\bar{\beta}}(TH) \right\} \right]^2 \times \left[\sum_{\alpha=e,\mu} \left\{ N_j^{\alpha\beta}(TH) + N_j^{\bar{\alpha}\bar{\beta}}(TH) \right\} \right]^{-1} \quad (\text{A1})$$

⁶ In this appendix, for simplicity we ignore the systematic errors, since our discussions are only qualitative to understand parameter degeneracy in the atmospheric neutrino measurements.

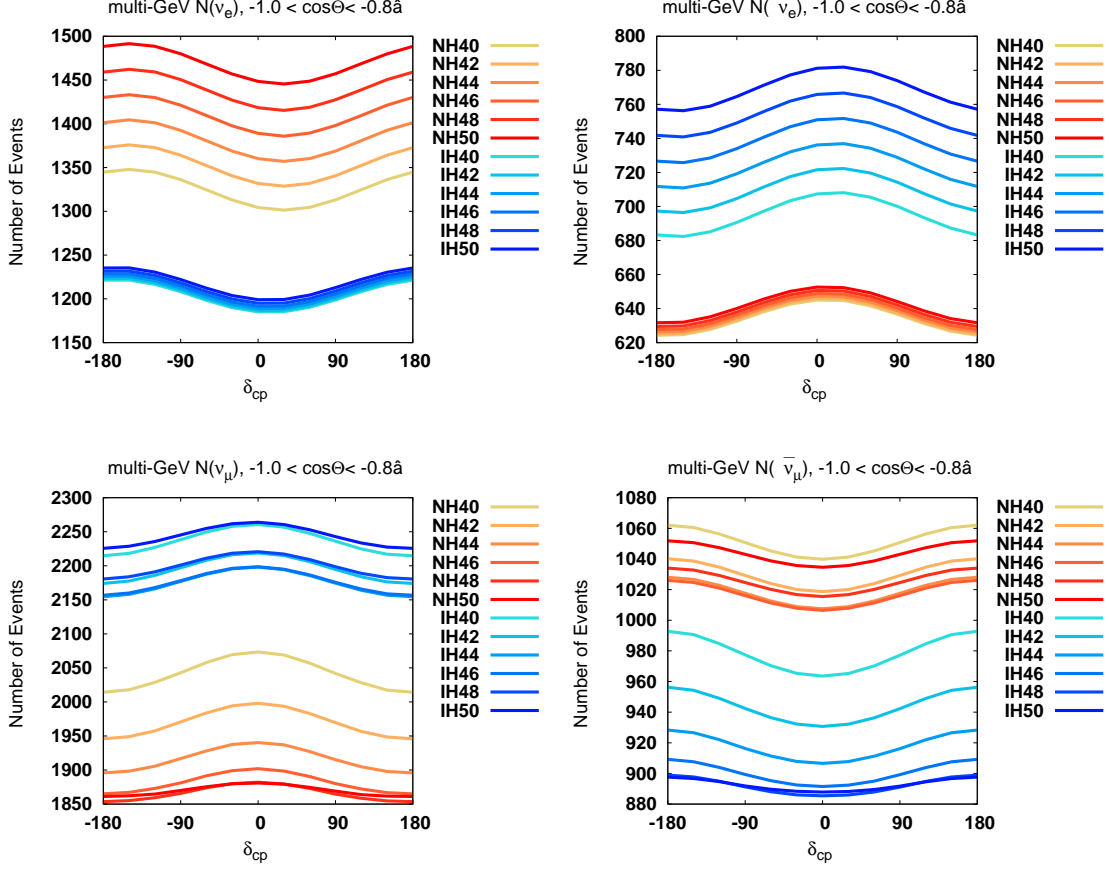


FIG. 10: The numbers of the multi-GeV events for the zenith angle $-1 < \cos \Theta < -0.8$. Left panels: neutrino events; Right panel: antineutrino events.

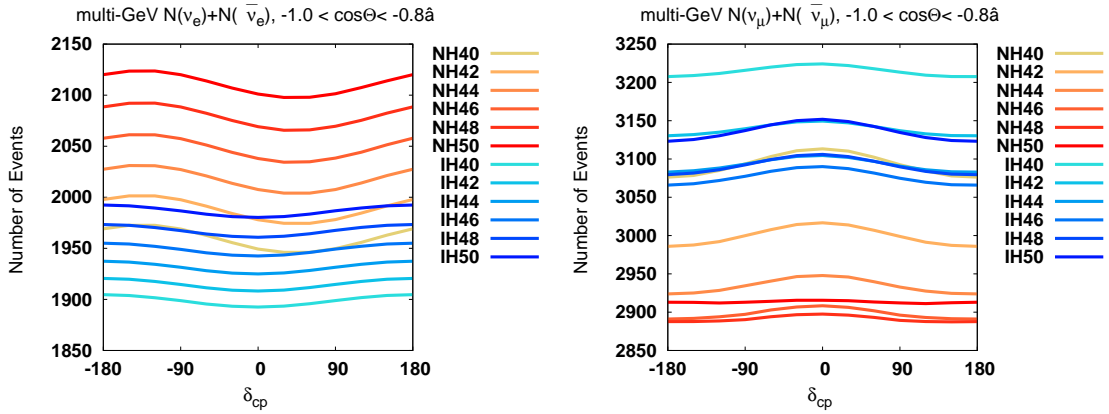


FIG. 11: The numbers of the multi-GeV events for the zenith angle $-1 < \cos \Theta < -0.8$. Left panel: $N(\nu_e \rightarrow \nu_e) + N(\nu_\mu \rightarrow \nu_e) + N(\bar{\nu}_e \rightarrow \bar{\nu}_e) + N(\bar{\nu}_\mu \rightarrow \bar{\nu}_e)$; Right panel: $N(\nu_e \rightarrow \nu_\mu) + N(\nu_\mu \rightarrow \nu_e) + N(\bar{\nu}_e \rightarrow \bar{\nu}_\mu) + N(\bar{\nu}_\mu \rightarrow \bar{\nu}_e)$

MH	$N_1^{\mu e}$	$N_1^{\bar{\mu} \bar{e}}$	N_1^{ee}	$N_1^{\bar{e} \bar{e}}$	$N_1^{e\mu}$	$N_1^{\bar{e}\bar{\mu}}$	$N_1^{\mu\mu}$	$N_1^{\bar{\mu}\bar{\mu}}$
NH	498 ± 108	66 ± 15	898 ± 1	$573 \pm 9 \times 10^{-2}$	11 ± 3	$2 \pm 5 \times 10^{-4}$	1970 ± 130	1040 ± 35
IH	118 ± 26	259 ± 56	1093 ± 1	$474 \pm 9 \times 10^{-1}$	41 ± 10	$3 \pm 5 \times 10^{-3}$	2180 ± 70	950 ± 65

TABLE II: The numbers of events for the zenith bin $j = 1$ ($-1.0 < \cos \Theta < -0.8$) with variations in θ_{23} and δ for each mass hierarchy.

where we have introduced the simplified notations

$$N_j^{\alpha\beta}(MH) \equiv F_0(\nu_\alpha) P(\nu_\alpha \rightarrow \nu_\beta, MH) \sigma(\nu_\beta)$$

$$N_j^{\bar{\alpha}\bar{\beta}}(MH) \equiv F_0(\bar{\nu}_\alpha) P(\bar{\nu}_\alpha \rightarrow \bar{\nu}_\beta, MH) \sigma(\bar{\nu}_\beta).$$

Here $F_0(\nu_\alpha)$ is the original flux of ν_α before oscillations, $P(\nu_\alpha \rightarrow \nu_\beta, MH)$ is the oscillation probability with a given Mass Hierarchy (either the True Hierarchy $MH = TH$ or the Wrong Hierarchy $MH = WH$), $\sigma(\nu_\beta)$ ($\sigma(\bar{\nu}_\beta)$) is the cross section for ν_β ($\bar{\nu}_\beta$) to produce the charged lepton ℓ_β^- (ℓ_β^+), and j stands for the index for the zenith angle bin $((j-6)/5 < \cos \Theta < (j-5)/5)$.

To see how degeneracy occurs, let us take a look, for simplicity, at the number of events for the zenith bin $j = 1$ ($-1.0 < \cos \Theta < -0.8$), in which the matter effect is expected to be important. Assuming that data is taken at Hyperkamiokande for 2000 days with 0.56 Mton fiducial volume, the numbers of events for each channel are estimated and are given in Table II. From these numbers of events we can understand that the main contribution for the μ -like events comes from the $\nu_\mu \rightarrow \nu_\mu$ channel, and that the main contribution for the e -like events comes from the $\nu_\mu \rightarrow \nu_e$ channel. For NH (IH) we have more events in the neutrino (antineutrino) mode. To understand these results qualitatively, we have to take into account a few facts. First of all, in the case of the normal (inverted) hierarchy, the oscillation probability $P(\nu_\mu \rightarrow \nu_e)$ ($P(\bar{\nu}_\mu \rightarrow \bar{\nu}_e)$) is enhanced due to the matter effect. Secondly, around the neutrino energy region $E \sim 10\text{GeV}$, the ratio of the atmospheric neutrinos for the zenith bin $j = 1$ ($-1.0 < \cos \Theta < -0.8$) is [44] $F(\nu_\mu):F(\bar{\nu}_\mu):F(\nu_e):F(\bar{\nu}_e) \simeq 40:40:10:7$. The reason that the μ/e ratio is high at $E \sim 10\text{GeV}$ is because muons do not have enough time to decay to produce e^\pm and ν_e or $\bar{\nu}_e$ at such a high energy. Thirdly, the ratio of the cross sections for ν_α and $\bar{\nu}_\alpha$ is approximately 2:1. Thus we have more numbers of events $N(\nu_\mu \rightarrow \nu_\alpha)$, rather than $N(\bar{\nu}_\mu \rightarrow \bar{\nu}_\alpha)$, $N(\nu_e \rightarrow \nu_\alpha)$ and $N(\bar{\nu}_e \rightarrow \bar{\nu}_\alpha)$, and the mass hierarchy should be the normal hierarchy to have enhancement for $N(\nu_\mu \rightarrow \nu_e)$.

In Fig. 10 we show the numbers of the multi-GeV events (e -like, μ -like) for the zenith angle $-1 < \cos \Theta < -0.8$, assuming that we can separate the neutrino and antineutrino modes. The left (right) panels are for the neutrino (antineutrino) modes. Because of the enhancement due to the matter effect, a remarkable dependence on θ_{23} as well as separation between the two mass hierarchies can be seen for NH (IH) in the neutrino (antineutrino) mode. These features can be seen for the zenith angle region $-1 < \cos \Theta \lesssim -0.4$. For the zenith angle region $\cos \Theta \gtrsim -0.4$, the matter effect is not so dramatic, and we do not have the distinction between the two mass hierarchies.

The qualitative behaviors in Fig. 10 can be roughly understood from the analytic expressions of the oscillation probabilities. Using the formalism by Kimura-Takamura-Yokomakura [51, 52] on the exact analytic expression for the oscillation probability in matter with constant density, it can be shown to first order in $|\Delta m_{21}^2 / \Delta m_{31}^2|$ and to arbitrary order in θ_{13} that the appearance and disappearance probabilities satisfy the following behaviors:

$$\begin{aligned} & P(\nu_\mu \rightarrow \nu_\mu; \theta'_{23}) - P(\nu_\mu \rightarrow \nu_\mu; \theta_{23}) \\ & \simeq (\sin^2 2\theta'_{23} - \sin^2 2\theta_{23}) \left\{ \cos^2 \tilde{\theta}_{13} \sin^2 \left(\frac{\Lambda_+ L}{2} \right) + \sin^2 \tilde{\theta}_{13} \sin^2 \left(\frac{\Lambda_- L}{2} \right) \right\} \\ & - (\sin^4 \theta'_{23} - \sin^4 \theta_{23}) \sin^2 2\tilde{\theta}_{13} \sin^2 \left(\frac{\Delta \tilde{E}_{31} L}{2} \right), \end{aligned} \quad (\text{A2})$$

$$P(\nu_\mu \rightarrow \nu_e; \theta'_{23}) - P(\nu_\mu \rightarrow \nu_e; \theta_{23}) \simeq (\sin^2 \theta'_{23} - \sin^2 \theta_{23}) \sin^2 \left(\frac{\Delta \tilde{E}_{31} L}{2} \right), \quad (\text{A3})$$

where we have introduced the following notations (G_F is the Fermi coupling constant and N_e is the density of electrons):

$$\begin{aligned} \Delta E_{jk} & \equiv \frac{\Delta m_{jk}^2}{2E} \equiv \frac{m_j^2 - m_k^2}{2E}, \quad A \equiv \sqrt{2} G_F N_e, \\ \Delta \tilde{E}_{31} & \equiv \{ (\Delta E_{31} \cos 2\theta_{13} - A)^2 + (\Delta E_{31} \sin 2\theta_{13})^2 \}^{1/2}, \\ \Lambda_\pm & \equiv \frac{\Delta E_{31} + A \pm \Delta \tilde{E}_{31}}{2}, \quad |\tilde{U}_{\mu 1}|^2 \simeq \frac{\Delta E_{31} (\Lambda_+ - \Delta E_{31})}{2 \Delta \tilde{E}_{31} \Lambda_-}, \\ |\tilde{U}_{\mu 3}|^2 & \simeq \frac{\Delta E_{31} (\Delta E_{31} - \Lambda_-)}{2 \Delta \tilde{E}_{31} \Lambda_+}, \quad \tan 2\tilde{\theta}_{13} \equiv \frac{\Delta E_{31} \sin 2\theta_{13}}{\Delta E_{31} \cos 2\theta_{13} - A} \end{aligned}$$

For example, near the resonance where the $\tilde{\theta}_{13}$ is close to 45° , from Eq. (A2) we see in the case of NH that the $\sin^4 \theta_{23}$ terms becomes dominant, and the behavior is consistent with the bottom panels of Fig. 10. From the plot we see that the behaviors of the neutrino events are opposite to

that of the antineutrino events. If one had a charge identification of the events, then one could resolve the wrong hierarchy - wrong octant degeneracy.

In Fig. 11 we show the numbers of the multi-GeV events (e -like, μ -like), in which the neutrino and antineutrino events are combined together, as is done in most of the data of water Čerenkov detectors. From this plot it is easy to see that the NH - LO solution is confused with the IH - HO solution for both the e -like and μ -like events. Since the variation of the numbers of events with respect to θ_{23} is smaller in IH than in NH, the minimum value of hierarchy χ^2 is expected to be larger in the case of $TH = NH$ than in the case of $TH = IH$. This implies that the significance of the mass hierarchy is larger in the case of $TH = NH$ than in the case of $TH = IH$.

-
- [1] F. P. An et al. (Daya Bay), Phys. Rev. Lett. **115**, 111802 (2015), 1505.03456.
 - [2] Y. Abe et al. (Double Chooz Collaboration), JHEP **1410**, 86 (2014), 1406.7763.
 - [3] J. H. Choi et al. (RENO), Phys. Rev. Lett. **116**, 211801 (2016), 1511.05849.
 - [4] F. Capozzi, G. L. Fogli, E. Lisi, A. Marrone, D. Montanino, and A. Palazzo, Phys. Rev. **D89**, 093018 (2014), 1312.2878.
 - [5] D. V. Forero, M. Tortola, and J. W. F. Valle, Phys. Rev. **D90**, 093006 (2014), 1405.7540.
 - [6] J. Bergstrom, M. C. Gonzalez-Garcia, M. Maltoni, and T. Schwetz, JHEP **09**, 200 (2015), 1507.04366.
 - [7] J. Burguet-Castell, M. B. Gavela, J. J. Gomez-Cadenas, P. Hernandez, and O. Mena, Nucl. Phys. **B608**, 301 (2001), hep-ph/0103258.
 - [8] H. Minakata and H. Nunokawa, JHEP **10**, 001 (2001), hep-ph/0108085.
 - [9] G. L. Fogli and E. Lisi, Phys. Rev. **D54**, 3667 (1996), hep-ph/9604415.
 - [10] V. Barger, D. Marfatia, and K. Whisnant, Phys. Rev. **D65**, 073023 (2002), hep-ph/0112119.
 - [11] M. Ghosh, P. Ghoshal, S. Goswami, N. Nath, and S. K. Raut, Phys. Rev. **D93**, 013013 (2016), 1504.06283.
 - [12] M. Ghosh, P. Ghoshal, S. Goswami, and S. K. Raut, Phys. Rev. **D89**, 011301 (2014), 1306.2500.
 - [13] M. Ghosh, P. Ghoshal, S. Goswami, and S. K. Raut, Nucl. Phys. **B884**, 274 (2014), 1401.7243.
 - [14] M. Ghosh, Phys. Rev. **D93**, 073003 (2016), 1512.02226.
 - [15] K. Abe et al. (T2K), PTEP **2015**, 043C01 (2015), 1409.7469.
 - [16] D. Ayres et al. (NOvA Collaboration) (2007).
 - [17] S. Ahmed et al. (ICAL) (2015), 1505.07380.

- [18] A. Chatterjee, P. Ghoshal, S. Goswami, and S. K. Raut, JHEP **06**, 010 (2013), 1302.1370.
- [19] A. Ghosh, T. Thakore, and S. Choubey, JHEP **04**, 009 (2013), 1212.1305.
- [20] A. Stahl et al. (2012), CERN-SPSC-2012-021, SPSC-EOI-007.
- [21] M. Ghosh, P. Ghoshal, S. Goswami, and S. K. Raut, JHEP **03**, 094 (2014), 1308.5979.
- [22] M. G. Aartsen et al. (IceCube PINGU) (2014), 1401.2046.
- [23] S. Choubey and A. Ghosh, JHEP **11**, 166 (2013), 1309.5760.
- [24] M. Blennow and T. Schwetz, JHEP **09**, 089 (2013), 1306.3988.
- [25] W. Winter, Phys. Rev. **D88**, 013013 (2013), 1305.5539.
- [26] R. Acciarri et al. (DUNE) (2015), 1512.06148.
- [27] V. Barger, A. Bhattacharya, A. Chatterjee, R. Gandhi, D. Marfatia, and M. Masud, Phys. Rev. **D89**, 011302 (2014), 1307.2519.
- [28] V. Barger, A. Bhattacharya, A. Chatterjee, R. Gandhi, D. Marfatia, and M. Masud, Int. J. Mod. Phys. **A31**, 1650020 (2016), 1405.1054.
- [29] M. Ghosh, S. Goswami, and S. K. Raut, Eur. Phys. J. **C76**, 114 (2016), 1412.1744.
- [30] K. Abe et al. (Hyper-Kamiokande Working Group) (2014), 1412.4673.
- [31] K. Abe, T. Abe, H. Aihara, Y. Fukuda, Y. Hayato, et al. (2011), 1109.3262.
- [32] J. Cao et al. (ICFA Neutrino Panel) (2015), 1501.03918.
- [33] S. Prakash, S. K. Raut, and S. U. Sankar, Phys. Rev. **D86**, 033012 (2012), 1201.6485.
- [34] S. K. Agarwalla, S. Prakash, and S. U. Sankar, JHEP **07**, 131 (2013), 1301.2574.
- [35] T. Kajita (2016), Talk given at 1st Atmospheric Neutrino Workshop, Cluster of Excellence, Garching, Germany, February 2016.
- [36] P. Huber, M. Lindner, and W. Winter, Comput. Phys. Commun. **167**, 195 (2005), hep-ph/0407333.
- [37] P. Huber, J. Kopp, M. Lindner, M. Rolinec, and W. Winter, Comput. Phys. Commun. **177**, 432 (2007), hep-ph/0701187.
- [38] S. Fukasawa and O. Yasuda, Adv. High Energy Phys. **2015**, 820941 (2015), 1503.08056.
- [39] R. Foot, R. R. Volkas, and O. Yasuda, Phys. Rev. **D58**, 013006 (1998), hep-ph/9801431.
- [40] O. Yasuda, Phys. Rev. **D58**, 091301 (1998), hep-ph/9804400.
- [41] O. Yasuda (2000), hep-ph/0006319.
- [42] Y. Fukuda et al. (Super-Kamiokande), Phys. Rev. Lett. **81**, 1562 (1998), hep-ex/9807003.
- [43] M. Honda, T. Kajita, K. Kasahara, and S. Midorikawa, Phys. Rev. **D52**, 4985 (1995), hep-ph/9503439.
- [44] M. Honda, M. Sajjad Athar, T. Kajita, K. Kasahara, and S. Midorikawa, Phys. Rev. **D92**, 023004

- (2015), 1502.03916.
- [45] Y. Ashie et al. (Super-Kamiokande), Phys. Rev. **D71**, 112005 (2005), hep-ex/0501064.
- [46] S. Fukasawa and O. Yasuda, Nucl. Phys. **B914**, 99 (2017), 1608.05897.
- [47] H. Nunokawa, S. J. Parke, and R. Zukanovich Funchal, Phys.Rev. **D72**, 013009 (2005), hep-ph/0503283.
- [48] F. Capozzi, E. Lisi, and A. Marrone, Phys. Rev. **D91**, 073011 (2015), 1503.01999.
- [49] O. Yasuda, New J. Phys. **6**, 83 (2004), hep-ph/0405005.
- [50] H. Minakata, M. Sonoyama, and H. Sugiyama, Phys. Rev. **D70**, 113012 (2004), hep-ph/0406073.
- [51] K. Kimura, A. Takamura, and H. Yokomakura, Phys. Lett. **B537**, 86 (2002), hep-ph/0203099.
- [52] K. Kimura, A. Takamura, and H. Yokomakura, Phys. Rev. **D66**, 073005 (2002), hep-ph/0205295.